S. M. Mahmoud, Z. W. Sun, B. B. Dally, Z. T. Alwahabi, P. R. Medwell and G. J. Nathan
The effect of exit strain rate on soot volume fraction in turbulent non-premixed jet flames

http://hdl.handle.net/2440/102209

The Effect of Exit Strain Rate on Soot Volume Fraction in Turbulent Non-Premixed Jet Flames

S. M. Mahmoud [a], Z. W. Sun [a], B. B. Dally [a], Z. T. Alwahabi [b], P. R. Medwell [a] and G. J. Nathan [a]

Schools of [a] Mechanical and [b] Chemical Engineering

Centre for Energy Technology, University of Adelaide, S.A. 5005, AUSTRALIA

saleh.mahmoud@adelaide.edu.au

Abstract

Laser-Induced Incandescence (LII) measurements from soot were conducted in three attached turbulent non-premixed jet flames spanning various locations in each flame. The effect of the variation of the strain rate on soot behaviour is assessed through the comparison of the mean and integrated data for the three flames. The change is strain rate was achieved through the simultaneous variation of the jet burner diameter and the fuel exit velocity at the nozzle, thus allowing a systematic study of the influence of the exit strain rate in turbulent combustion while keeping the exit Reynold's number constant. These measurements, which are part of an ongoing comprehensive study of the effect of strain rate on mean, instantaneous, integrated soot volume fraction as well as intermittency data, reveal an inverse relationship between the exit strain rate with the mean and instantaneous soot volume fraction (SVF), and agree with radiation tests performed previously for the same flames.

Introduction

Soot is one of the key features of many combustion systems since it plays a significant and a highly effective role in radiative heat transfer [1,2]. The complex processes of soot formation and oxidation in flames are governed by interdependent parameters such as fuel type, strain rate, pressure, temperature, and mixing rate [3]. Importantly, many of these dependencies are coupled in the presence of turbulence. The effect of the local flame strain rate on soot formation has been investigated in various studies, but mostly in laminar flames because such flames allow stable and well-defined conditions that are not achievable in turbulent conditions. These studies found out that both soot concentration and soot zone thickness decrease with increasing flame strain rate [4-6]. However, in turbulent sooty flames the measurements of strain rate are predominantly limited to characteristic, or global, rather than local values due to the difficulties of performing such measurements in unsteady flames containing soot.

Qamar *et al.* [7] measured the soot volume fraction in three different turbulent diffusion flames using laser-induced incandescence (LII). Their work provided insight into the effect of global mixing rate on the instantaneous local and the average soot volume fraction. The global mixing rate calculated by Qamar *et al.* is defined as the inverse global residence time, and is calculated as the volume flow rate of fuel divided by the flame volume [7, 8]. Their measurements reveal an inverse relationship between global mixing rate and both the total amount of soot in the flame and local instantaneous soot volume fractions, broadly consistent with trends in laminar flames. Qamar *et al*. work, despite

its significance, was performed on three different burners albeit with similar operating conditions. Their measurements do not provide information on the dependency of the exit strain rate or the Reynolds number, which together characterize the mixing processes, as well as the soot formation and evolution processes. Kent and Bastin [9] investigated the effect of mixing in acetylene turbulent jet flames from simple pipe nozzles and showed that the average soot volume fraction decreases with increasing characteristic strain rate. Additionally, the rate of this decrease is higher at high mixing rates than at low mixing rates. Noteworthy is that, soot extinction which is a line-of-sight technique was used for their measurement, thus limiting the data presented to averaged values with no information about the local soot in the flames. Besides, stabilizers were added some distance from the nozzle to the flames with high Reynolds number, which would interfere with the flame chemical and physical scales.

The three-dimensional and unsteady nature of turbulent flames makes it highly desirable to provide measurements in multiple dimensions, allowing the acquisition of spatially correlated scalars and their gradients which influence soot evolution [10]. In order to allow the joint application of experiments and computational fluid dynamics, from which the major advances in combustion research have been derived, it is necessary for the experiments to be performed under very well characterized conditions. In a similar vein, owing to the complexity of soot evolution in turbulent flames, it is desirable that measurements be performed in attached turbulent

flames, since lifted flames are not only more difficult to predict but also strongly inhibit soot formation through partial premixing. Hence for this purpose, LII imaging of soot in a series of five attached turbulent non-premixed jet flames was performed and some preliminary results are present in this paper. The effect of two parameters, the exit strain rate and the exit Reynolds number, was assessed in this study. The exit strain rate was defined as the ratio of the exit fuel velocity to the exit jet diameter, and is assessed separately through a simultaneous variation of the jet burner diameter and the fuel exit velocity at the nozzle. This variation allows a systemic study of the influence of the aforesaid parameter in turbulent combustion through isolating its effects. While the results presented here are preliminary and restricted to strain rate effect, detailed results of the study will be reported in the near future. This study aims at contributing towards achieving a better understanding of soot evolution in turbulent flames by the joint application of high fidelity databases and model development.

Experimental Setup

Flames

Three attached turbulent non-premixed jet flames were used in this study. The jet flames burn an identical mixture of ethylene-hydrogen-nitrogen at 40-41-19 percent composition by volume, respectively, with co-flowing air at ambient temperature and atmospheric pressure. Full details of the flame conditions are provided in Table 1. Time-averaged photographs with long-time exposures of flames 1 to 3 are presented in Figure 1. Ethylene (C_2H_4) was selected as the fuel to examine soot formation and destruction due to its relatively well-defined chemistry and high soot yields. Hydrogen (H_2) was premixed with ethylene in order to keep the flames attached at high Reynolds numbers. Nitrogen (N_2) was also added as a diluent to achieve a high Reynolds number and higher stoichiometric mixture fraction through increasing
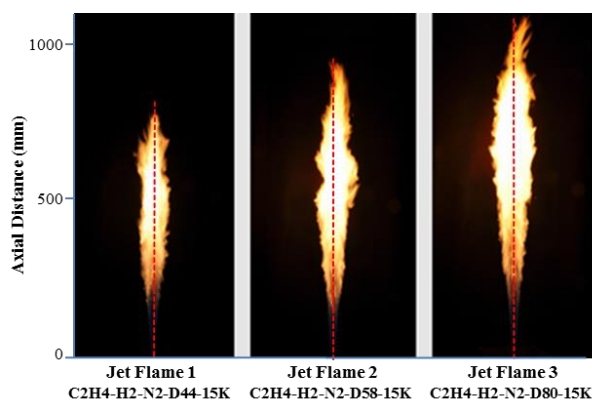
Reynolds number, as well as to influence soot formation through thermal means. Flames from this set have been employed in previous studies, such in simultaneous planar measurements of temperature and soot concentration by the authors [11] and a study of the global characteristics of hydrogen–hydrocarbon blended fuels by Dong *et al*. [12].

Burners

The burners used to stabilise the flames comprise a set of round aluminium tube of 4.4 mm, 5.8 mm, and 8 mm ID, with a tapered end and a wall thickness of 1 mm each. The pipes were mounted in the centre of a contraction delivering co-flowing air at ambient temperature and at a mean velocity of 1.1 m/s. The contraction has a square cross-section of dimensions 150 mm by 150 mm, and the pipe jet burner outlet rises above the contraction edge by a distance of 18 mm. A traverse was used to move the burner and contraction vertically through the optical diagnostic beams to enable measurements throughout various heights of the entire flame.

The extraction hood was traversed with the flame to avoid any influence of the exhaust extraction on the flames. Measurements were performed at thirteen axial locations spanning most regions of the flame. Data from five axial locations, x/Lf= 0.24, 0.42, 0.61, 0.73 and 0.90, where x is the axial distance from the nozzle exit, as well as integrated data over full flame length are presented in this paper.

Laser Induced Incandescence (LII)

Soot concentration was measured quantitatively using the LII technique. Soot Incandescence was recorded on an ICCD camera and then converted to meaningful *SVF* data. Calibration for the LII technique was performed via soot extinction from an ethylene flat flame generated by a McKenna burner, using a CW DPSS laser at 1064 nm. LII was performed with a pulsed Nd:YAG laser at 1064 nm, while the incandescence was collected with an ICCD camera through a 430-nm (10 nm bandwidth) interference filter. This arrangement was selected to suppress the C_2 laser-induced emission and to minimize interference from flame radiation [13]. The gate-width of the LII camera was set to 50 ns, while the timing was set to coincide with the LII excitation, as this has been proven to decrease the sensitivity of the signal to the soot particle size [14]. The LII laser sheet was approximately 24 mm high and 500 μm thick and captures the full flame width. The laser fluence was kept above 0.5 J/cm^2, in the plateau region of the LII response curve, to minimize any influence on the LII signal due to fluence variation from attenuation or from beam "steering". The influence of beam steering and signal trapping on the accuracy of soot volume

Fig 1. Photographs of the attached jet flames 1 to 3, from left to right, respectively. Dashed red line corresponds to the centreline location. Each photograph is 500 mm width by 1100 mm height.

Table 1. Flow conditions of the attached jet flames

Flame name		Central Jet Diameter (D)	Average Exit Velocity (U)	Exit Strain Rate (U/D)	Exit Reynolds Number	Visible Flame Length
		(mm)	(m/sec)	(s^{-1})	(-)	(mm)
C2H4-H2-N2-D44-15K	**Flame 1**	4.4	56.8	12,900	15,000	750
C2H4-H2-N2-D58-15K	**Flame 2**	5.8	42.4	7,300	15,000	975
C2H4-H2-N2-D80-15K	**Flame 3**	8	31.5	4,000	15,000	1190

fraction has been fully investigated in turbulent non-premixed sooting flames by Sun *et al.* [15]. The maximum "steering" of the laser beams in the flames was measured to be 2 milli-rad, corresponding to a 50% increase in the laser sheet thickness from one side of the flame to the other. This in turn leads to the spatial resolution in the out-of-plane direction varying from 300 to 450 μm throughout the flame. The data was binned over 3 pixels in height and width, resulting in a final volume imaged by each binned pixel being 0.72 x 0.72 x 0.75 mm for all measurements.

Results

A comparison of the axial-radial distribution of the mean and the room mean square (RMS) of the SVF in parts per billion (ppb), collected from 500 instantaneous images, is presented in Figure 2.

The minimum detection limit is 20 ppb, while the uncertainty in the measurements is calculated to be 20%. At any given height, from $x/L_f = 0.1$ throughout to the flame tip region, a consistent trend of soot radial distribution within the three flames is found, where more soot is found in flames with lower exit strain rate, a trend noticeable for both mean and RMS data. It is observed that the maximum mean soot volume fraction, for the three flames, occurs on the nozzle axis, while its axial location is consistent for the three flames ($x/L_f \sim 0.60$). This is consistent with the trends in radiant heat profiles for the same profiles reported by Xue *et al.*, where the peak heat flux from the flames was found in the downstream region of $0.6 < x/L_f < 0.7$ [12], confirming the significant role of soot in flame radiation and temperature. It is also close to the SVF peak at $x/L_f = 0.6$ reported for the simple jet flame measured by Qamar *et al.* [7].
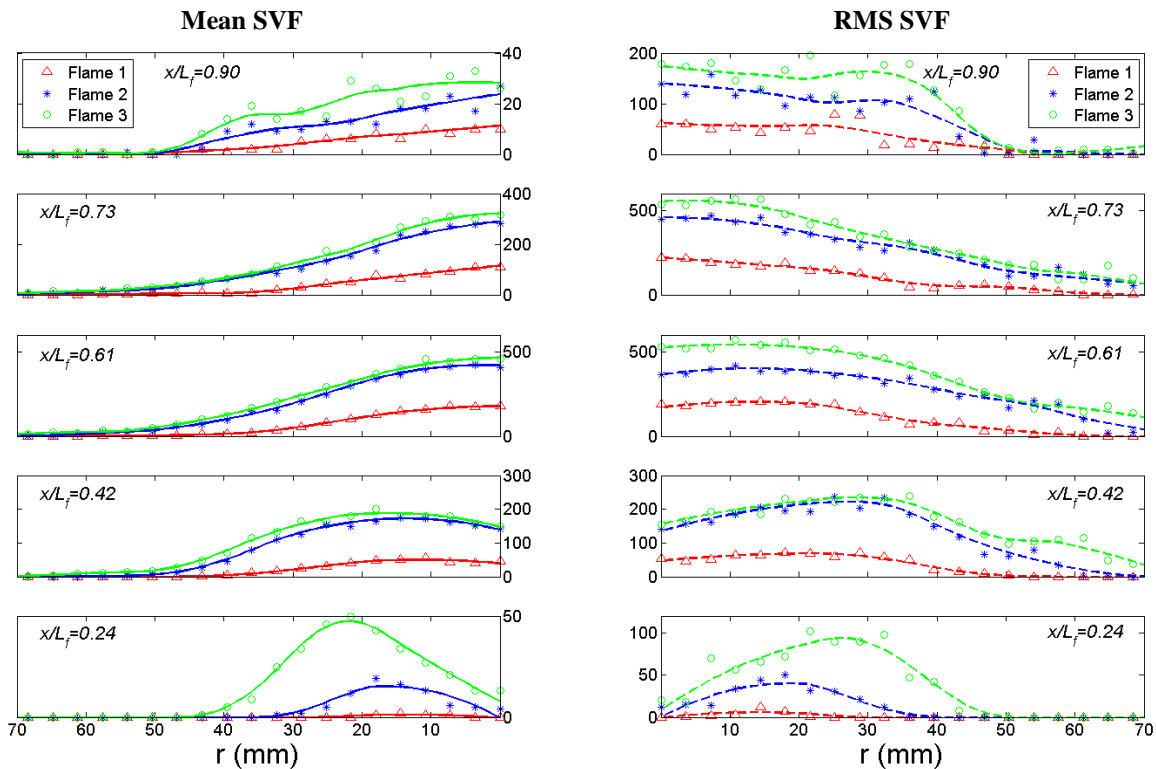

Fig 2. Mean and RMS radial profiles of soot volume fraction, at various downstream locations. Mean profiles of flames 1-3 is on the left side, RMS profiles on the right side. Flames 1, 2 and 3 have the same Reynolds number (15,000) and different exit strain rates of 12,900, 7,300 and 4,000 sec^{-1} respectively. Measurements were conducted across the full flame width. Profiles for one side of the flames are presented since symmetry tests for all flames showed good results.
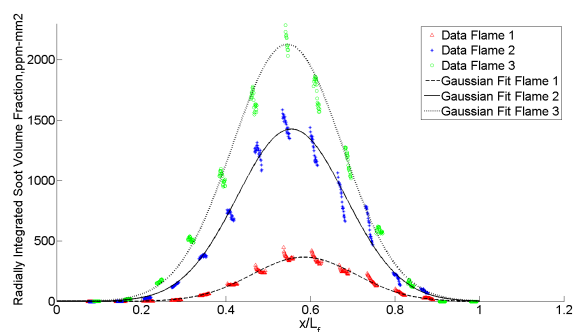
Fig 3. Axial profiles of radially integrated SVF, in ppm, over full flame length. Markers represent experimental data, while the profiles are Gaussian fits for the experimental data.

Fig 4. Integrated SVF over full flame volume. Markers represent values of integrated data. Curve plot is an exponential function of the integrated data.

High RMS values for SVF are reported throughout the flame, owing to large fluctuations of soot concentration. Higher ratio of RMS to mean SVF values is observed at far downstream and upstream location measurements, indicating high intermittency at these locations.

Total soot per axial length is measured by integrating mean SVF over the cross-section of the flame at each axial height. The integrated values, which have the units of soot volume per unit length, are presented in Figure 3. These results show a similar trend of the inverse relationship between exit strain rate and integrated SVF in the mean and RMS data. The data was fitted with a Gaussian distribution function with R^2 value of 0.98. Consistent with Figure 2, the location of peak SVF for all flames is in the range of $0.56 < x/Lf < 0.58$.

Figure 4 presents total soot per unit volume of each flame, calculated by estimating the area under the Gaussian curve plots from radially integrated SVF over non-normalized flame length (plots are not presented here). It is deduced from figure 4 that flame 3 has about 1.8 more soot than flame 2, which in turn has 5 times more soot than flame 1. The data points were then fitted with an exponential curve function, with an R^2 value of 0.90. This function is chosen since the volume integrated SVF is predicted to peak at very low strain rates and is predicted to decay with increasing exit strain rate. The reciprocal fit, while plausible, can be used to predict the total amount of soot concentration for various strain rates, for turbulent non-premixed flames of similar composition and exit flow conditions. A detailed analysis of the effect of the strain rate on the mean, integrated, and instantaneous SVF, as well as intermittency studies is currently underway, and will be presented in future publications.
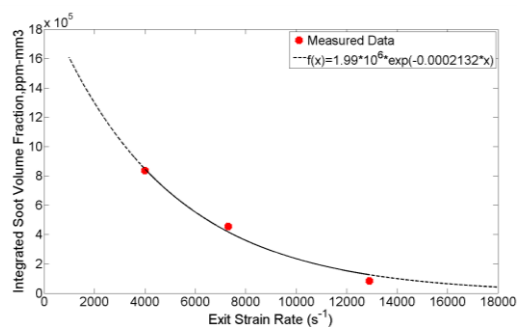
Conclusions

Preliminary results of the effect of varying the exit strain rate on soot behaviour in turbulent diffusion flames are presented. These results reveal an inverse relationship between SVF and exit strain rate and shows consistency of the mean and integrated SVF profiles which peak at the same location for all flames investigated in this study, and with radiation heat profiles from literature. Further analysis will follow in upcoming publications.

References

1. C. R. Shaddix and T. C. Williams, *Am. Sci.* **95**, 232–239 (2007).
2. D.W. Dockery and P. H. Stone, *N. Engl. J. Med.* **356**, 511–513 (2007).
3. J.H. Kent, D. Honnery, *Combust. Sci. Technol.* **54**, 383–397 (1987).
4. M.E. Decroix, W.L. Roberts, *Combust. Sci. Technol.* **160**, 165–189 (2000).
5. A. Beltrame, P. Porshnev, W. Merchan-Merchan, A. Saveliev, A. Fridman, L.A. Kennedy, O. Petrova,S. Zhdanouk, F. Amouri, O. Charon, *Combust. Flame* **124**, 295–310 (2001).
6. H. Wang, D.X. Du, C.J. Sung, C.K. Law, *Proc.Combust. Inst.* **26** (1996) 2359–2368.
7. N.H. Qamar, G.J. Nathan, Z.T. Alwahabi, D.K. King, *Proc. Combust.* Inst. **30** (2005) 1493–1500.
8. S.R. Turns, F.H. Myhr, Combust. Flame 87 (1991) 319–335.
9. J.H. Kent, S.J. Bastin, *Combust. Flame* **56,** 29–42 (1984).
10. R.S. Barlow, *Proc. Combust. Inst.* **31**, 49–75 (2007).
11. S.M. Mahmoud, G.J. Nathan, P.R. Medwell et al, *Proc.Combust. Inst.*, **35**, 1931-1938 (2015).
12. X. Dong, G.J. Nathan, S. Mahmoud, P.J. Ashman, D. Gu, B.B. Dally, *Combust. Flame* **162**, 1326–1335 (2015).
13. C. Schulz, B.F. Kock, M. Hofmann, et al. *Appl.Phys.* B **83**, 333–354 (2006).
14. R.L. Vander Wal, *Appl. Opt.* **35,** 6548–6559 (1996).
15. Z. W. Sun, Z. T. Alwahabi, D. H. Gu, S. M. Mahmoud, G. J. Nathan, B. B. Dally, *Appl. Phys. B*, DOI 10.1007/s00340-015-6080-6.